Identification of the 1,3,2,4-Dithiadiazolyl RCNSNS• Radical Dimers in Solution, Their Dimeric Concerted Photochemically Symmetry-Allowed Rearrangement to 1,2,3,5-Dithiadiazolyl RCNSSN• by the Net Exchange of Adjacent Cyclic Sulfur and Nitrogen Atoms, and the Photolysis of RCNSNS•

Jack Passmore* and Xiaoping Sun

Department of Chemistry, University of New Brunswick, Fredericton, NB, Canada E3B 6E2

Received July 27, 1995[⊗]

The 1,3,2,4-dithiadiazolyl RCNSNS• radicals undergo an unprecedented concerted rearrangement to the thermodynamically more stable 1,2,3,5-dithiadiazolyl RCNSSN• radicals by the net exchange of adjacent cyclic sulfur and nitrogen atoms. The UV−visible spectra of RCNSNS• (R = Ph, *p*-$O_2NC_6H_4$, 3,5-$(O_2N)_2C_6H_3$, CF_3) in solution show bands at 250 nm (strong) and 680 nm (very weak) attributable to monomer and two dimer bands at 376 and 480 nm, the positions of which are independent of the substituents, providing direct identification of the radical dimers in solution. The dimerization equilibrium constant ($K_{298} \simeq 0.7$ for R = Ph) at room temperature was derived from the enthalpy and entropy changes for the dimerization of PhCNSNS• ($\Delta H_d° = -19.0$ kJ/mol, $\Delta S° = -66.5$ J/mol) estimated by a variable-temperature ESR spectroscopic study. In addition, RCNSNS• (R = Bu^t, Ph) undergo an apparent unimolecular photolysis to RCN and possibly SNS• (analogue of ONO•). The photochemical rearrangement and dissociation (for R = Ph and 3,5-$(O_2N)_2C_6H_3$) were shown to proceed by irradiation of the radical dimer (376 and 480 nm) and monomer (250 nm), respectively. Thus, the radical rearrangement reasonably occurs via a concerted dimeric pathway shown by molecular orbital calculations (CNDO) to be photochemically symmetry-allowed. In addition, we propose that the radical dissociation proceeds via a concerted unimolecular photochemically symmetry-allowed process.

Introduction

SNS^+ undergoes a quantitative symmetry-allowed cycloaddition reaction with nitriles leading to the 6π 1,3,2,4-dithiadiazolylium $RCNSNS^+$.[1] We have shown that reduction of the cation in dilute solution leads to quantitative formation of the 7π 1,3,2,4-dithiadiazolyl RCNSNS• (**A**) radical (R = CH_3,[1a] CF_3,[2] Bu^t,[3] and 2,5-$Me_2C_6H_3$, Ph, *p*-$O_2NC_6H_4$, and 3,5-$(O_2N)_2C_6H_3$[1f]) detected by ESR spectroscopy. In some cases, we have isolated the radical in pure form (R = CH_3 (at low temperature),[2] Bu^t,[3] Ph,[1f] *p*-$O_2NC_6H_4$[1f]). Since then, the diradicals $(CNSNS)_2^{2•}$ [4] and *p*-$C_6H_4(CNSNS)_2^{2•}$ [5] and several related multiradicals (e.g. *m*-$C_6H_4(CNSNS)_2^{2•}$, 4,4′-•SNSNCC_6H_4−C_6H_4CNSNS•, and *sym*-$C_6H_3(CNSNS)_3^{3•}$)[6] have been isolated. However, we have found that, depending on the nature of the substituent group R and the experimental conditions, RCNSNS• (**A**) rearranged[2,3] to the thermodynamically more stable isomer 1,2,3,5-dithiadiazolyl RCNSSN• (**B**).[7a−c] Thus an unprecedented isomerization had occurred in which the cyclic sulfur and nitrogen atoms had switched positions. In dilute solutions (ca. 10^{-2} M), when R is CH_3,[2] Bu^t,[3] or Ph,[1f] the rearrangement only takes place under exposure to the light, but when R is more electronegative, e.g. CF_3[2] or 3,5-$(O_2N)_2C_6H_3$,[1f] the rearrangement also occurs in the dark but qualitatively more slowly.[1f] The rearrangement of RCNSNS• (at a given concentration) appears to be qualitatively faster the higher the electronegativity of the substituent group R. RCNSSN• (R = Bu^t,[3] CF_3,[2] Ph,[1f]

* To whom the correspondence should be addressed.

[⊗] Abstract published in *Advance ACS Abstracts,* January 1, 1996.

(1) (a) MacLean, G. K.; Passmore, J.; Rao, M. N. S.; Schriver, M. J.; White, P. S.; Bethell, D.; Pilkington, R. S.; Sutcliffe, L. H. *J. Chem. Soc., Dalton trans.* **1985**, 1405. (b) MacLean, G. K.; Passmore, J.; Schriver, M. J.; White, P. S.; Bethell, D.; Pilkington, R. S.; Sutcliffe, L. H. *J. Chem. Soc., Chem. Commun.* **1983**, 807. (c) Burford, N.; Johnson, J. P.; Passmore, J.; Schriver, M. J.; White, P. S. *J. Chem. Soc., Chem. Commun.* **1986**, 966. (d) Passmore, J.; Schriver, M. J. *Inorg. Chem.* **1988**, *27*, 2749. (e) Parsons, S.; Passmore, J.; Schriver, M. J.; Sun, X. *Inorg. Chem.* **1991**, *30*, 3342. (f) Passmore, J.; Sun, X.; Parsons, S. *Can. J. Chem.* **1992**, *70*, 2972. (g) Parsons, S.; Passmore, J. *Acc. Chem. Res.* **1994**, *27*, 101.

(2) Burford, N.; Passmore, J.; Schriver, M. J. *J. Chem. Soc., Chem. Commun.* **1986**, 140.

(3) Brooks, W. V. F.; Burford, N.; Passmore, J.; Schriver, M. J.; Sutcliffe, L. H. *J. Chem. Soc., Chem. Commun.* **1987**, 69.

(4) (a) Parsons, S.; Passmore, J.; White, P. S. *J. Chem. Soc., Dalton Trans.* **1993**, 1499. (b) Brooks, V. F. W.; Brownridge, S.; Parsons, S.; Passmore, J. *Phosphorus, Sulfur Silicon Relat. Elem.* **1994**, *93*−*94*, 43.

(5) Banister, A. J.; Rawson, J. M.; Clegg, W.; Birkby, S. L. *J. Chem. Soc., Dalton Trans.* **1991**, 1099.

(6) (a) Aherne, C.; Banister, A. J.; Luke, A. W.; Rawson, J. M.; Whitehead, R. J. *J. Chem. Soc., Dalton Trans.* **1992**, 1277. (b) Banister, A. J.; Lavender, I.; Rawson, J. M.; Clegg, W.; Tanner, B. K.; Whitehead, R. J. *J. Chem. Soc., Dalton Trans.* **1993**, 1421.

(7) (a) Vegas, A.; Perez-Salazar, A.; Banister, A. J.; Hey, R. G. *J. Chem. Soc., Dalton Trans.* **1980**, 1812. (b) Banister, A. J.; Hansford, M. I.; Hauptman, Z. V.; Wait, S. T. *J. Chem. Soc., Dalton Trans.* **1989**, 1705. (c) Hofs, H.-U.; Bats, J. W.; Gleiter, R.; Hartmann, G.; Mews, R.; Eckert-Maksic, M.; Oberhammer, H.; Sheldrick, G. M. *Chem. Ber.* **1985**, *118*, 3781. (d) Cordes, A. W.; Liblong, S. W.; Phillips, S. G.; Oakley, R. T. *Inorg. Chem.* **1989**, *28*, 4147. Boere, R. T.; Cordes, A. W.; Oakley, R. T. *J. Am. Chem. Soc.* **1987**, *109*, 7781. Bestari, K. T.; Boere, R. T.; Oakley, R. T. *J. Am. Chem. Soc.* **1989**, *111*, 1579. (e) Bestari, K.; Oakley, R. T. *Can. J. Chem.* **1991**, *69*, 94.

0020-1669/96/1335-1313$12.00/0

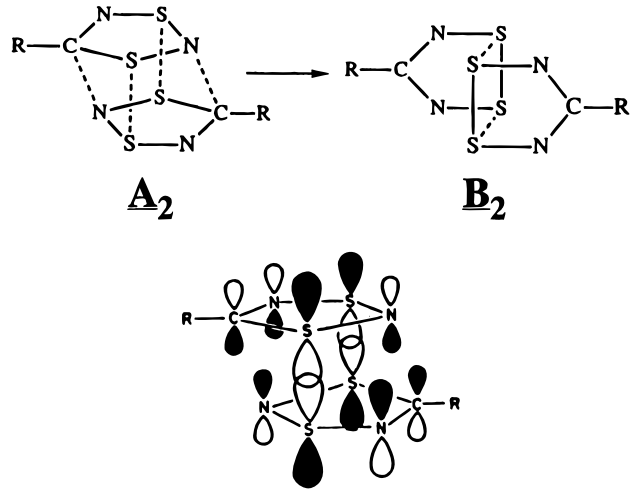

Figure 1. Dimeric pathway for the rearrangement of $RC\overline{NSNS}^{\bullet}$ to $RC\overline{NSSN}^{\bullet}$ and the SOMO of $(HC\overline{NSNS}^{\bullet})_2$ dimer (CNDO).

$3,5\text{-}(O_2N)_2C_6H_3$[1f]) were prepared in essentially quantitative yield by this facile rearrangement. Oakley has identified two other types of rearrangements, i.e. the so-called "1,3-nitrogen shift" reaction[7d] and the skeletal scrambling of sulfur diimide radical anions.[7e] In a preliminary communication,[2] we reported that the rearrangement of $RC\overline{NSNS}^{\bullet}$ to $RC\overline{NSSN}^{\bullet}$ was second order in radical concentration (R = CH_3) as determined by the half-life method using ESR spectroscopy, and the rearrangement was proposed to proceed by the formation of $\pi^*-\pi^*$ dimer $\mathbf{A}_2$, which by a small displacement of appropriate atoms led to the formation of the related $\pi^*-\pi^*$ dimer $\mathbf{B}_2$ (Figure 1). In a second preliminary communication,[3] we demonstrated that the rearrangement was photochemically induced, and from a CNDO study of the two proposed dimers, we proposed that the rearrangement was "thermally forbidden" but "photochemically symmetry allowed". More recently, Banister and co-workers[6a] reported that crystalline $p\text{-}C_6H_4(C\overline{NSNS})_2^{2\bullet}$ thermally rearranges to the corresponding disulfide at 150 °C. The $p\text{-}C_6H_4\text{-}(C\overline{NSNS})_2^{2\bullet}$ units in the structure are linked through $\pi^*-\pi^*$ interactions in a head to tail fashion in an infinite polymeric arrangement.[5] The rearrangement was envisaged to occur by a pathway similar to that we previously proposed.[2,3] In this paper the UV−visible and ESR spectroscopic studies of the dimerization of $RC\overline{NSNS}^{\bullet}$ in solution and a photolytic study of the rearrangement of $RC\overline{NSNS}^{\bullet}$ to $RC\overline{NSSN}^{\bullet}$ are reported. In addition, the discovery of the photolysis of $RC\overline{NSNS}^{\bullet}$ to RCN and another primary intermediate product reasonably proposed to be $SNS^{\bullet}$ (analogue of $ONO^{\bullet}$) is reported, and a possible mechanism of the photolysis is presented.

Experimental Section

General Methods, Instrumentation, and Starting Materials. The sources of chemicals and acquisition of ESR (first derivative; utilizing 4 mm quartz tubes to reduce microwave absorption by SO_2 solvent) and NMR (^1H, ^{13}C) spectra have been described elsewhere.[1f] The UV−visible spectra were recorded with a Hewlett-Packard 8452A spectrophotometer. The photolyses of radical samples at individual wavelengths 376, 480, and 680 nm were performed by using the light source of a Perkin-Elmer 330 spectrophotometer (slit width 6 nm). The photolyses at 254 nm were obtained by using a 140 W Hanovia Hg lamp. $RC\overline{NSNS}AsF_6$ (R = Bu^t, CF_3, Ph, $3,5\text{-}(O_2N)_2C_6H_3$) and pure solid radicals $RC\overline{NSNS}^{\bullet}$ (R = Ph, $p\text{-}O_2NC_6H_4$) and $PhC\overline{NSSN}^{\bullet}$ were prepared as described.[1f,2,3] The solvents $CFCl_3$ and liquid SO_2 were dried over molecular sieves and CaH_2, respectively, and well degassed. The manipulations on the radical samples prior to the photolyses were carried out in the dark and under strictly anhydrous conditions with all volatiles and solids manipulated in the vacuum line and drybox, respectively.[8]

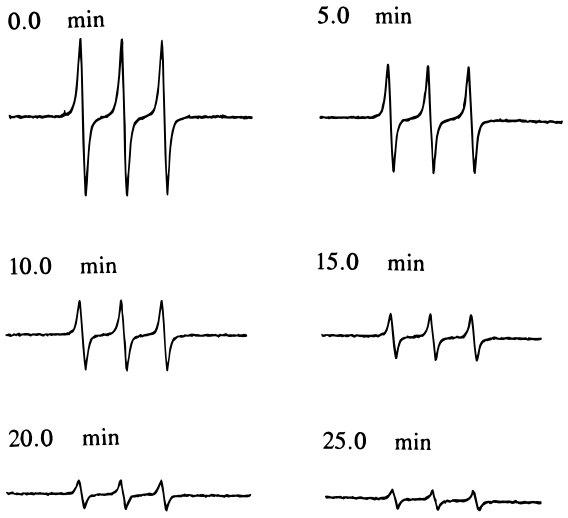

Figure 2. ESR spectra of $Bu^t\overline{CNSNS}^{\bullet}$ as a function of irradiation (at 254 nm) time.

Kinetic Study of the Photolysis of $Bu^t\overline{CNSNS}^{\bullet}$ by ESR Spectroscopy. A $Bu^t\overline{CNSNS}^{\bullet}$ sample was prepared in a glass-blown vessel incorporating a glass bulb (10 cm^3, equipped with a J. Young Teflon-stemmed Pyrex valve) and an attached ESR tube separated by a coarse or medium glass frit which were thoroughly flame-dried. SO_2 (2 g) was condensed at −196 °C onto a solid mixture of $Bu^t\overline{CNSNS}AsF_6$ (0.0046 g, 0.013 mmol), $SbPh_3$ (0.010 g, 0.028 mmol), and Me_4NCl (0.010 g, 0.092 mmol) which were loaded into the bulb through the stem of the valve by removal of the Teflon stem[8] and using a hand made glass funnel (here and elsewhere). After the reduction was completed, the SO_2 was removed by evacuation at −15 °C and $CFCl_3$ (12.84 g) added, giving a $Bu^t\overline{CNSNS}^{\bullet}$ solution (1.5×10^{-3} M) on mixing. The ESR tube was washed with three aliquots of solution and then partially filled and flame-sealed at −196 °C (here and elsewhere). The sample was quickly warmed to room temperature and irradiated by UV light at 254 nm. ESR spectra were recorded as a function of the irradiation time (Figure 2). The peak height of the original three-line pattern signal of $Bu^t\overline{CNSNS}^{\bullet}$ [3] decreased as the photolysis proceeded, but the line width did not change and no other signals were observed. Therefore the concentration of radical was proportional to peak height (h) (most upfield peak).[9] After 35 min, the solution was pale yellow over a yellow precipitate, and the original signal had almost disappeared. The log *h* vs *t* (irradiation time) curve was established by linear regression analysis, showing a good (correlation coefficient 0.998) linear relationship (Supporting Information Figure S1).

(8) Murchie, M.; Passmore, J. In *Inorganic Syntheses*; Shreeve, J. M., Ed.; Wiley: New York, 1986; Vol. 24. Murchie, M.; Passmore, J.; Kapoor, R.; Schatte, G. In *Inorganic Syntheses*; Cowley A. H., Ed.; Wiley: New York, 1996; Vol. 31, in press.

(9) The intensity of an ESR signal (the first derivative of an absorption band) can be expressed as $I = (\text{constant})h(\Delta H_{pp})^2$, which is directly proportional to the concentration of a radical species. Here *h* stands for the peak height (arbitrary unit) and ΔH the "peak−peak" width (in gauss). See: Wertz, J. E.; Bolton, J. R. *Electron Spin Resonance Elementary Theory and Practical Applications*; McGraw-Hill Inc.: New York, 1972; pp 32−36. Poole, C. P., Jr. *Electron Spin Resonance: A Comprehensive Treatise on Experimental Techniques*; John Wiley and Sons Inc.: New York, 1983; pp 466−477.

Characterization of the Products of the Photolysis of Bu^{t}CNSNS$^\bullet$ by NMR (^{1}H, ^{13}C) Spectroscopy. Two Bu^{t}CNSNS$^\bullet$ samples in $CFCl_3$ were prepared essentially as described above. For the ^{1}H NMR study, Bu^{t}CNSNSAsF$_6$ (0.060 g, 0.17 mmol), $SbPh_3$ (0.060 g, 0.17 mmol), and Me_4NCl (0.060 g, 0.55 mmol) gave a Bu^{t}CNSNS$^\bullet$ solution (0.2 M) in a 5 mm NMR tube; and for the ^{13}C NMR study, Bu^{t}CNSNSAsF$_6$ (0.408 g, 1.17 mmol), $SbPh_3$ (0.34 g, 0.96 mmol), and Me_4NCl (0.040 g, 3.67 mmol) gave a Bu^{t}CNSNS$^\bullet$ solution (0.5 M) in a 10 mm NMR tube. The Bu^{t}CNSNS$^\bullet$ samples in $CFCl_3$ solution were irradiated at 254 nm for 1 h (^{1}H NMR sample) and 3 h (^{13}C NMR sample), giving yellow solutions over a yellow precipitate (S_8, FT-Raman). ^{1}H NMR, δ (ppm): 7.23 (m, int 7%, $SbPh_3$), 1.42 (s, int 13%), 1.38 (s, int 13%), 1.32 (s, int 100%, Bu^{t}CN). ^{13}C NMR, δ (ppm): 142−130 (a group of peaks due to $SbPh_3$ and $SbPh_3Cl_2$), 125 (Bu^{t}CN, C_{CN}), 29.5 (Bu^{t}CN, C_{CH_3}), 29.0 (Bu^{t}CN, tert-C). The assignments of ^{1}H and ^{13}C resonances to Bu^{t}CN were made by comparison of the chemical shifts with those of standard Bu^{t}CN reagent in $CFCl_3$.

Determination of the Enthalpy ($\Delta H_d°$) and Entropy ($\Delta S_d°$) of the Dimerization of PhCNSNS$^\bullet$ in Solution by Variable-Temperature ESR Spectroscopy. The PhCNSNS$^\bullet$ sample was prepared essentially as described for Bu^{t}CNSNS$^\bullet$. A mixture of SO_2 (0.055 g) and $CFCl_3$ (1.417 g) was condensed onto a solid mixture of PhCNSNSAsF$_6$ (0.0139 g, 0.0376 mmol), $SbPh_3$ (0.053 g, 0.15 mmol), and Me_4NCl (0.031 g, 0.28 mmol), giving a PhCNSNS$^\bullet$ solution (0.0380 M). The ESR spectra were recorded at +20, +5, −10, −25, −40, −55, and −70 °C, exhibiting only 1:1:1 triplet signals in all cases (Supporting Information Figure S2), showing that no rearrangement has occurred. The concentrations of PhCNSNS$^\bullet$ monomer at various temperatures were determined by comparing the intensity (I)[9] of the most upfield peak (the line width of which changed with temperature) of the 1:1:1 triplet curve with that (I_0) of the corresponding peak for the spectrum measured at +20 °C using the relationship $C = C_0I/I_0$, and the initial concentration of PhCNSNS$^\bullet$ (0.0380 M) was taken as the reference concentration (C_0) of PhCNSNS$^\bullet$ monomer at 20 °C, assuming that the dimerization at this temperature was negligible (ca. 4%).[10a] The concentrations of the (PhCNSNS$^\bullet$)$_2$ dimer at various temperatures were then determined by difference.[10b] The enthalpy ($\Delta H_d°$) and entropy ($\Delta S_d°$) of the dimerization of PhCNSNS$^\bullet$ in solution were determined from the gradient and intercept of the ln K vs $1/T$ curve (Supporting Information Figure S3, correlation coefficient 0.98), respectively, where K and T are the dimerization equilibrium constant and absolute temperature (in K) respectively. $\Delta H_d° = -19.0(2)$ kJ/mol and $\Delta S_d° = -66.5(7)$ J/mol. The equilibrium constant (K_{298}) of the dimerization of PhCNSNS$^\bullet$ at 298 K was estimated to be ca. 0.72 on the basis of the $\Delta H_d°$ and $\Delta S_d°$ values, very similar to that found for PhCNSSN$^\bullet$.[10b] A correction for the ESR signal intensity with temperature was not made, which, however, has been shown to be negligibly small for the $CFCl_3$ solvent by Sutcliffe.[10c] Full experimental details are included in Supporting Information Tables S1 and S2.

UV−Visible Spectroscopic and Photolytic Studies on RCNSNS$^\bullet$ (R = Ph, *p*-$O_2NC_6H_4$, 3,5-$(O_2N)_2C_6H_3$, CF_3). The samples of radicals for UV−visible spectroscopic and photolytic studies were prepared in a vessel incorporating a Pyrex bulb (10 cm^3) and a 0.1 cm path length quartz UV cell connected via a glass frit. The vessel (except the UV cell) was flame-dried before use. For each sample of RCNSNS$^\bullet$ (R = Ph, *p*-$O_2NC_6H_4$), the solutions at various concentrations were prepared by dissolving freshly prepared solid RCNSNS$^\bullet$[1f] (kept at −70 °C before use in order to prevent any rearrangement) in a preweighed quantity of $CFCl_3$ in the bulb (resulting in specific concentrations of RCNSNS$^\bullet$). The UV cell was washed with the solution three times, and part of the solution was then poured back into the UV cell for the UV−visible spectroscopic measurements. The photolyses of the PhCNSNS$^\bullet$ samples at 254 nm (mercury lamp) and at 376, 480, and 680 nm (Perkin-Elmer spectrophotometer) were performed in the UV cell in situ. For 3,5-$(O_2N)_2C_6H_3$CNSNS$^\bullet$ (0.02 M), the sample was prepared in a similar vessel with an attached ESR tube by reducing 3,5-$(O_2N)_2C_6H_3$-CNSNSAsF$_6$ (0.016 g, 0.035 mmol) with excess $Na_2S_2O_4$ (0.016 g, 0.092 mmol) in SO_2 in the dark at room temperature, followed by careful removal of the SO_2 at 0 °C and addition of preweighed $CFCl_3$ (2.28 g). Part of the solution was then poured into the UV cell, and the UV−visible measurements and the photolytic experiment at 376 nm were performed in the same way as described for PhCNSNS$^\bullet$. The photolyzed radical solution was then poured into the ESR tube for a subsequent ESR measurement. For CF_3CNSNS$^\bullet$, the sample was prepared by reducing CF_3CNSNSAsF$_6$ (0.011 g, 0.030 mmol) with excess $SbPh_3$ (0.023 g, 0.065 mmol) in the presence of Me_4NCl (0.018 g, 0.17 mmol) in preweighed SO_2 (0.91 g) in the dark at room temperature. Part of the solution was transferred into the UV cell, and a UV−visible spectrum (Hewlett-Packard spectrophotometer) was recorded.

Molecular Orbital Calculations. The electronic structures of the HCNSNS$^\bullet$ radical monomer as a model for RCNSNS$^\bullet$, HCN as a model for RCN, and SNS$^\bullet$ were calculated at the *ab initio* STO-3G (RHF for HCN and ROHF for HCNSNS$^\bullet$ and SNS$^\bullet$) level with the GAUSSIAN-86 suite of programs[11] using the geometry of the appropriate fragment in *p*-$C_6H_4(CNSNS)_2^{2\bullet}$,[5] the experimental geometry of HCN,[12] and the optimized geometry of SNS$^\bullet$,[13] respectively. The electronic structures of (HCNSNS$^\bullet$)$_2$ and (HCNSSN$^\bullet$)$_2$ radical dimers (as models for dimers $\mathbf{A}_2$ and $\mathbf{B}_2$, respectively) were calculated at the CNDO level, using the experimental geometries for the appropriate portions of the related radical dimers ($C_6H_4S_2N^\bullet)_2$[14] and (PhCNSSN$^\bullet$)$_2$.[7a]

Results and Discussion

UV−Visible Spectra of RCNSNS$^\bullet$ and RCNSSN$^\bullet$ Radicals: Direct Observation of the (RCNSNS$^\bullet$)$_2$ Dimers in Solution. The UV−visible spectra of blue PhCNSNS$^\bullet$ solutions at different concentrations were recorded in the range 200−700 nm (Figure 3). The PhCNSNS$^\bullet$ sample at 0.024 M exhibits

(10) (a) The percentage of dimerization (ca. 4%) was obtained by using the estimated equilibrium constant (0.72) at 298 K (see below). (b) Fairhurst, S. A.; Johnson, K. M.; Sutcliffe, L. H.; Preston, K. F.; Banister, A. J.; Hauptman, Z. V.; Passmore, J. *J. Chem. Soc., Dalton Trans.* **1986**, 1465. (c) Fairhurst, S. A.; Steward, N. J.; Sutcliffe, L. H. *Magn. Reson. Chem.* **1987**, *25*, 60.

(11) Frisch, M.; Binkley, J. S.; Schegel, H. B.; Raghavachari, K.; Martin, R.; Stewart, J. P. P.; Defrees, D.; Seeger, R.; Whiteside, R.; Fox, D.; Fludel, E.; Pople, J. A. *GAUSSIAN 86*; Department of Chemistry, Carnegie-Mellon University: Pittsburgh, PA, 1986.

(12) Greenwood, N. N.; Earnshaw, A. *Chemistry of Elements*; Pergammon Press: New York, 1984; p 337.

(13) Optimized geometry of SNS$^\bullet$: $d_{S-N} = 1.546$ Å and ∠SNS = 151.3°. See: Yamaguchi, Y.; Xie, Y.; Grev, R. S.; Schaefer, H. F. *J. Chem. Phys.* **1990**, *92*, 3683.

(14) (a) Awere, E. G.; Burford, N.; Mailer, C.; Passmore, J.; Schriver, M. J.; White, P. S.; Banister, A. J.; Oberhammer, H.; Sucliffe, L. H. *J. Chem. Soc., Chem. Commmun.* **1987**, 66. Schriver, M. Ph.D. Thesis, University of New Brunswick, 1988. (b) Wolmershauser, G.; Kraft, G. *Chem. Ber.* **1990**, *123*, 881. (c) Awere, E. G.; Burford, N.; Mailer, C.; Passmore, J.; Schriver, M. J.; White, P. S.; Banister, A. J.; Oberhammer, H.; Sutcliffe, L. H. *J. Chem. Soc., Chem. Commun.* **1987**, 66. Awere, E. G.; Burford, N.; Haddon, R. C.; Parsons, S.; Passmore, Waszczak, J. V.; White, P. S. *Inorg. Chem.* **1990**, *29*, 4821.

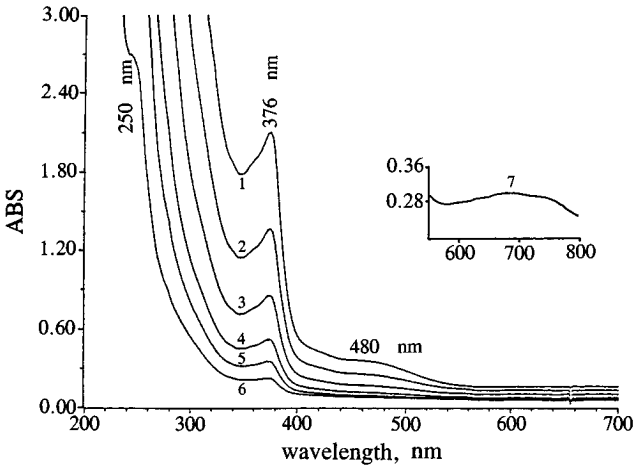

Figure 3. UV−visible spectra of PhCNSNS• in $CFCl_3$ at various concentrations: 1, 0.0883 M; 2, 0.0677 M; 3, 0.0524 M; 4, 0.0406 M; 5, 0.0317 M; 6, 0.0240 M. The inset spectrum (7) shows a broad absorption band (600−800 nm) of a sample at ca. 0.2 M.

two characteristic absorption bands centered at 250 nm (strong) and 376 nm (weak) at room temperature with a very poorly resolved band at higher energy. As the concentration increases, another very weak broad absorption band centered at 480 nm is observed. Highly concentrated solutions (0.2 M) are intensely blue and show a very weak and broad absorption band centered at 680 nm (extinction coefficient ca. 20)[15] which is likely responsible for the blue appearance of the solutions. The UV−vis spectrum of the disulfide isomer PhCNSSN• (ca. 0.04 M, yellow) showed an absorption band at 250−340 nm (Supporting Information Figure S4) corresponding to the yellow color of the solution. The bands responsible for the colors of both radicals likely originate from $\pi-\pi$ and/or $\pi^*-\pi^*$ transitions.

The absorbances (ABS) of PhCNSNS• samples at 376 and 480 nm in the original UV−vis spectra (Figure 3) show linear relationships with the square of the radical concentration, $[PhCNSNS•]^2$ (Figure 4). These spectra were simulated by computer (Quattro Pro). Figure 5 shows one simulated spectrum (0.0240 M; 6 in Figure 3), indicating that the original band centered at 376 nm (Figure 3) may consist of two superimposed bands centered at 360 and 376 nm, respectively. In addition, another band centered at 280 nm was resolved. The absorbances of the three bands at 280, 360, and 376 nm in the simulated spectra were shown to be directly proportional to the square of the PhCNSNS• concentration, $[PhCNSNS•]^2$ (Supporting Information Figure S5). These results unambiguously show that all four of the bands at 280, 360, 376, and 480 nm originate from the absorptions of a radical dimer $(PhCNSNS)_2$ which is in an equilibrium with the radical monomer PhCNSNS• in solution (eq 1) and whose (dimer) concentration is shown to be directly

$$2PhCNSNS• \rightleftharpoons (PhCNSNS)_2 \qquad (1)$$

proportional to the square of the monomer concentration,

(15) Various SNS• based radicals exhibit blue colors. For example, $CF_3CSNSCCF_3$• has a weak and broad absorption at 708 nm ($\epsilon = 80$) giving rise to an intensely blue appearance, similar to the situation for PhCNSNS•. See: Schriver, M. J. *Ph.D. Thesis*, University of New Brunswick, 1988. Passmore, J.; Schriver, M. J. Manuscript in preparation.

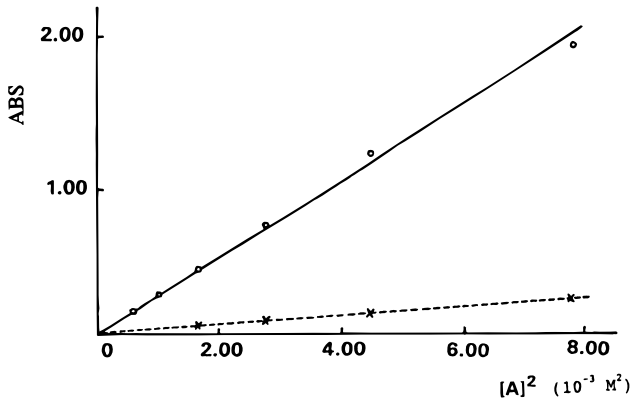

Figure 4. Relationship between the absorbances of PhCNSNS• in $CFCl_3$ at 376 nm ($(ABS)_{376}$, solid line] and 480 nm [$(ABS)_{480}$, dotted line) and the square of the initial concentration of the PhCNSNS• (**A**) monomer, $[\mathbf{A}]^2$.

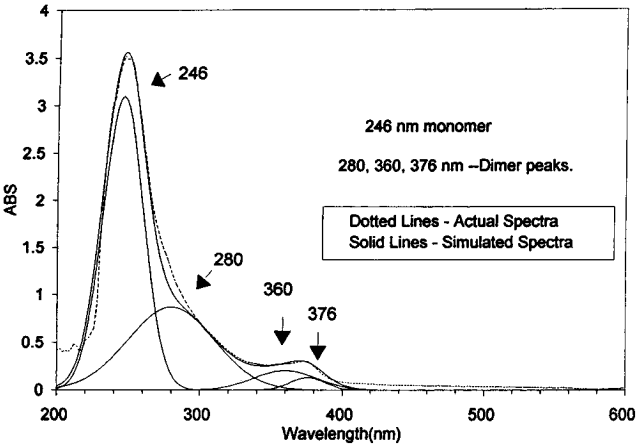

Figure 5. Computer-simulated UV−visible spectrum of PhCNSNS• (0.0240 M).

$[PhCNSNS•]^2$, at a given temperature on the basis of the dimerization equilibrium (eq 1). In addition, the absorbance of the high-energy band at 246 nm in the simulated spectra was directly proportional to the PhCNSNS• concentration (cf. the band at 250 nm in the original spectrum (6 in Figure 3)), showing that it originates from a transition of the radical monomer from its ground state likely to a dissociative excited state (Figure 6 and below). The weak band at 680 nm is also very likely due to the monomer.

The UV−vis spectra of 0.02 M samples of RCNSNS• (R = *p*-$O_2NC_6H_4$, 3,5-$(O_2N)_2C_6H_3$) showed two characteristic absorption bands at essentially the same positions as those of PhCNSNS•, i.e. a strong monomer band centered at 250 nm and a weak dimer band at 376 nm; the weak band at 480 nm not visible at this concentration. For CF_3CNSNS•, the dimer absorption band was also observed at 376 nm. The monomer band at 250 nm was obscured by the solvent SO_2 (showing strong absorption below 340 nm).[16] The results imply that the energy levels of RCNSNS• MO's are likely independent of the

(16) The rearrangement of CF_3CNSNS• to CF_3CNSSN• took place during the attempted replacement of SO_2 with $CFCl_3$. On removal of SO_2, the concentration of dimer increases, thus increasing the rate of rearrangement. Therefore, the UV−vis spectrum of CF_3CNSNS• was directly recorded in SO_2 solution.

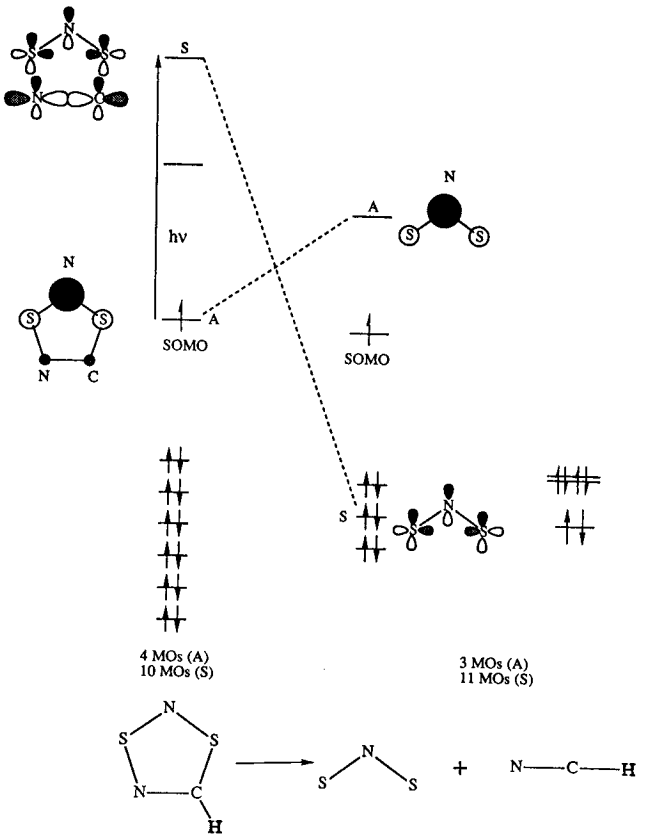

Figure 6. Correlation diagram of the molecular orbitals (STO-3G) of HCNSNS• and its photolysis products HCN and SNS·. The low-lying and some high unoccupied orbitals are omitted.

electronic nature of the substituents. Small differences in absorbances of the 376 and 480 nm bands for the RCNSNS• with different substituents are observed, and they may relate to the previously observed dependence of the completion time for the rearrangement of RCNSNS• on the nature of the R groups.[1f] The total amount of the (RCNSNS•)$_2$ dimer[17a] and/or the ratio of the trans $\mathbf{A}_2$ to other possible rotomers in cis and staggered configurations (see below) may increase as the electronegativity of R increases. Sutcliffe[17b] claimed that the dimerization of 1,2,3,5-dithiadiazolyl RCNSSN• radicals is greater for the more electronegative fluoro derivatives than for the corresponding less electronegative hydrogen analogue from his ESR studies and from comparison of the relative length of intermonomeric S···S interactions within the dimer. On this basis, it appears that, for the RCNSNS• radicals, the higher the electronegativity of R (indicated by the greater IP of RCN), the greater the extent of dimerization of RCNSNS•.[17] To our knowledge, this is the first UV−visible spectroscopic study of the dithiadiazolyl RCNSNS• or RCNSSN• radicals.

The dimerization of PhCNSNS• (eq 1) was further studied by variable-temperature ESR spectroscopy. The enthalpy and entropy changes for this radical dimerization are estimated to be $\Delta H_d^\circ = -19.0$ kJ/mol and $\Delta S_d^\circ = -66.5$ J/mol, respectively. The dimerization equilibrium constant at room temperature (298 K) is estimated to be approximately 0.72. On this basis, the extinction coefficients of the (PhCNSNS•)$_2$ dimer at several peak wavelengths (nm) are estimated (wavelength (extinction coefficient)):[17c] 280 (64 000), 360 (2400), 376 (2300), 480 (450).

Photolysis of Bu^{t}CNSNS•. On irradiation with UV light at 254 nm, Bu^{t}CNSNS• undergoes photolysis to give Bu^{t}CN (identified by NMR (^{1}H, ^{13}C)) and S_8 (FT-Raman). The ESR kinetic study showed that, on photolysis at this wavelength, the concentration of Bu^{t}CNSNS• (represented by the peak height (*h*) of the spectra) decayed as a function of time (a linear relationship between log *h* and *t*), showing the overall photolysis to be an apparent first-order process with respect to Bu^{t}CNSNS• concentration. No other signals were observed in the ESR spectra; therefore, rearrangement of Bu^{t}CNSNS• to Bu^{t}CNSSN• did not occur. The preliminary kinetic results are consistent with a unimolecular dissociation as shown by eq 2, although

$$\text{Bu}^t\text{CNSNS}^\bullet \rightarrow \text{Bu}^t\text{CN} + \text{SNS}^\bullet \qquad (2)$$

the detailed photochemical mechanism for this reaction cannot be established by the available data. The Bu^{t}CN was experimentally identified; therefore, the other primary intermediate product from the photodissociation can be reasonably identified as SNS• (cf. ONO•), which likely rapidly decomposes to sulfur and nitrogen under the photolysis conditions.

A similar unimolecular dissociation of RCNSNS• (R = Ph, *p*-$O_2NC_6H_4$) to RCN and SNS• in the mass spectrometer under electron impact is evidenced by the presence of SNS^+ and RCN^+ in their mass spectra[1f] at low voltage. In addition, the thermolyses of *p*-$O_2NC_6H_4$CNSNS•[1f] and •SNSNCCNSNS•[4] give *p*-$O_2NC_6H_4CN$ (IR) and •NSSNCCN[4] presumably due to the loss of SNS• and the subsequent rearrangement (for •NSSNCCN). A related unimolecular dissociation is observed for neutral cyclic PhCNNSN to give PhCN and NSN.[18] SNS• has been identified at 12 K from the products generated in an Ar matrix by discharge of a mixture of N_2 and CS_2.[19]

Photolytic Studies of RCNSNS•. In order to determine the major wavelengths which induce the photodissociation of RCNSNS• and the photochemical rearrangement of RCNSNS• to RCNSSN• and to further investigate the photolyses related to RCNSNS•, we carried out photolyses of PhCNSNS• at the absorptions observed in its UV−visible spectra, and the resulting

(17) (a) On the basis of high similarity of electronic structures and UV−visible spectra of RCNSNS• radicals, we assume that the extinction coefficients of a specific monomer or dimer absorption for RCNSNS• at a given wavelength are independent of the R groups. Given this assumption, the concentration of a radical dimer (RCNSNS•)$_2$ in solution is simply proportional to its absorbance at a given wavelength. (b) Fairhurst, S. A.; Sutcliffe, L. H.; Preston, K. F.; Banister, A. J.; Partington, A. S.; Rawson, J. M.; Passmore, J.; Schriver, M. J. *Magn. Reson. Chem.* **1993**, *31*,1027. (c) The concentration of the (PhCNSNS•)$_2$ dimer in equilibrium with the PhCNSNS• monomer (eq 1) at a given concentration in a dilute solution can be estimated by using the observed equilibrium constant (0.72). The extinction coefficients of several bands for the dimer absorptions were then estimated according to Beer's law.

(18) Wentrup, C.; Kambouris, P. *Chem. Rev.* **1991**, *91*, 363. Wentrup, C.; Fischer, S.; Maquestiau, A.; Flammang, R. *J. Org. Chem.* **1986**, *51*, 1908.

(19) The discharge of the mixture of N_2 and CS_2 in an Ar matrix gave more than 20 products (IR), including SNS•, NNS, NSS•, SN•, etc. See: Hassanzadeh, P.; Andrews, L. *J. Am. Chem. Soc.* **1992**, *114*, 83.

spectra were recorded. After a 0.02 M sample was photolyzed (Hg lamp) at 254 nm (monomer absorption) for 1.5 h, the characteristic absorption bands for PhCNSNS• at 250 and 376 nm disappeared and the UV spectrum showed the absorption band attributable to PhCN in ca. 90% yield presumably due to the elimination of SNS• (cf. the above photolysis of Bu^{t}CNSNS• and also see ref 1f). On photolysis (in a Perkin-Elmer 330 spectrophotometer) of similar samples (0.01 and 0.02 M) at 376 nm for 1.5 h, the characteristic absorption bands for PhCNSNS• at 250 and 376 nm disappeared with the appearance of an absorption band (250−340 nm) attributable to the disulfide isomer PhCNSSN•, indicating that essentially complete rearrangement had taken place in both cases. The UV−vis spectrum of a 0.02 M sample irradiated at 480 nm for 1.5 h remained unchanged, while a similar photolysis of a 0.06 M sample at 480 nm led to ca. 30% rearrangement (UV−vis), consistent with the absorbance at 480 nm being ca. one-tenth of that at 376 nm. The UV−vis spectrum of a sample (0.06 M) irradiated at 680 nm for 1.5 h remained unchanged. Similarly, photolysis of a 0.02 M sample of 3,5-$(O_2N)_2C_6H_3$CNSNS• at 376 nm (the dimer absorption) for 1.5 h led to only 3,5-$(O_2N)_2C_6H_3$CNSSN• (ESR). The above photolytic results indicate that the dimer absorption bands centered at 376 and 480 nm (Figure 3) are responsible for an apparently fast and slow photochemical rearrangement of RCNSNS• to RCNSSN•, respectively. The monomer band at 250 nm is responsible for the photodissociation of the radical PhCNSNS• to PhCN and SNS·. Our results indicate that the photochemical rearrangement of RCNSNS• to RCNSSN• in solution proceeds via an intermediate radical dimer (RCNSNS•)$_2$ at low concentration that is directly observed (for R = Ph, *p*-$O_2NC_6H_4$, 3,5-$(O_2N)_2C_6H_3$, and CF_3) by UV−visible spectroscopy.

Theoretical Analysis of the Photochemical Dissociation of RCNSNS• to RCN and SNS•. On the basis of a preliminary kinetic study of the overall photolysis of Bu^{t}CNSNS• (first order in the radical concentration), we reasonably propose that RCNSNS• undergoes unimolecular photochemical dissociation to RCN and SNS•. We assume that the dissociation of the planar HCNSNS• (C_s symmetry) proceeds along the molecule plane concertedly to give linear HCN[12] and angular SNS•,[13] and as a result, the three molecules are coplanar with retention of C_s symmetry throughout the dissociation process. Therefore we can correlate the MO's (STO-3G) of HCNSNS• with those of HCN and SNS• (Figure 6) according to the Woodward−Hoffmann rules.[20] Of the 14 occupied MO's (valence shell), for the reactant HCNSNS•, 10 are symmetric (S) and 4 are asymmetric (A); however, for the dissociation products HCN and SNS•, 11 are symmetric (S) and 3 are asymmetric (A). Therefore the correlation between MO's of the reactant and MO's of the products involves a crossover correlation; thus the dissociation is photochemically symmetry allowed but thermally symmetry forbidden. The SOMO of HCNSNS• (A) correlates with the LUMO of SNS• (A), and an occupied MO of SNS• (S) correlates with a high unoccupied MO of HCNSNS• (S), which is very likely dissociative due to the σ-antibonding component of the MO between the SNS and the CN fragments of the five-membered ring (see Figure 6). The transition from the SOMO (A) to the dissociative state (S) is symmetry allowed. As the unpaired electron is excited from the SOMO of HCNSNS• to its unstable dissociative state (250 nm, corresponding to 480 kJ/mol), a concerted and synchronous dissociation of HCNSNS• along its S−C and S−N bonds, giving linear HCN and angular SNS• (estimated to be very approximately 60 kJ/mol higher in total energy than HCNSNS• (Figure 7)[21]), may occur. Therefore, the absorption band of the RCNSNS• radical monomer at 250 nm (extinction coefficient ca. 1100 for R = Ph) can be reasonably assigned to this symmetry-allowed transition which is responsible for the photodissociation process leading to RCN, elemental sulfur, and N_2 (estimated to be very approximately 85 kJ/mol lower in total energy than HCNSNS• (Figure 7)[21]). The intermediate SNS• has been experimentally identified,[13,22] and its geometry was optimized at the TZ+2P-CISD level.[13] Thus, we have provided some experimental and theoretical evidence for the formation of SNS• from the direct photodis-

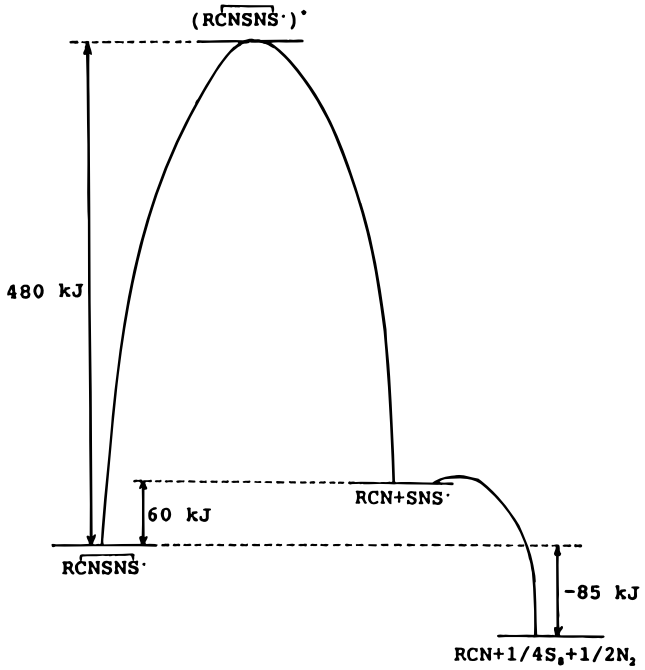

Figure 7. Schematic diagram of the energy change for the unimolecular photolysis of RCNSNS• to RCN and the intermediate SNS• and to final nitrile, sulfur, and nitrogen.

(20) Woodward, R. B.; Hoffmann, R. *The Conservation of Orbital Symmetry*; Academic Press: New York, 1970.

(21) The energy change is estimated from the difference in total bond energies of the corresponding reactants and products. The energy of the C−N bond in HCN is 887 kJ/mol. The energies of the C−N bond in HCN, the S−S bond in S_8, and the N−N bond in N_2 are 887, 226, and 941.69 kJ/mol, respectively. The energies of C−N, C−S, and S−S bonds in both HCNSNS• and HCNSSN• are 615 (for a C=N bond), 573 (for d_{CS} = 1.82 Å), and 424.7 (in S_8) kJ/mol, respectively. See: Huheey, J. E.; Keiter, E. A.; Keiter, R. L. *Inorganic Chemistry; Principles of Structure and Reactivity*; Harper Collins: New York, 1993; pp A21−A34. The energies of S−N bonds in all cases are calculated according to the equation $E(SN) = 2134.3 - 1126.4d_{SN}$ (kJ/mol). See: Parsons, S.; Passmore, J. *Inorg. Chem.* **1992**, *31*, 526. The S-N bond distances are as described in the Experimental Section for MO calculations.

(22) Amano, T.; Amano, T. *Abstracts of Papers*, 44th Symposium on Molecular Spectroscopy, June 12−16, 1989, Columbus, OH; Abstract RF1.

sociation of RCNSNS• radicals, which may be a cleaner source of SNS• than that reported in ref 19.

Mechanism of the Concerted Photochemically Symmetry-Allowed Bimolecular Rearrangement of RCNSNS• to RCNSSN•. It has been shown in this work that 2**A** is in equilibrium with $\mathbf{A}_2$, which we have identified in solution for R = Ph, *p*-$O_2NC_6H_4$, 3,5-$(O_2N)_2C_6H_3$, and CF_3, and a dimeric pathway has been established for the rearrangement of RCNSNS• to RCNSSN• by UV−vis spectroscopic studies. The X-ray crystal structures of the related species RCSNSCR• (R = CF_3,[14a] CN[14b]), $C_6H_4S_2N$•,[14c] and $(p\text{-}C_6H_4(CNSNS)_2^{2\bullet})_x$[5] showed intermolecular radical dimers formed via the S···S interactions in either a cis configuration ($CF_3CSNSCCF_3$• and NCCSNSCCN•) or a trans (head-to-tail) configuration ($C_6H_4S_2N$• and $(p\text{-}C_6H_4(CNSNS)_2^{2\bullet})_x$). In solution, the unrearranged radical dimers $(RCNSNS•)_2$ may possibly possess both a trans configuration $\mathbf{A}_2$ (Figure 1) and a cis configuration (180° rotomer of trans $\mathbf{A}_2$). Both configurations possess a $\pi^*-\pi^*$ structure formed by overlap of the monomer SOMO's on both sulfur atoms (two S···S contacts). In addition, a staggered dimer (cf. the twisted $(CF_3CNSSN•)_2$ dimer[7c]) with a single S···S contact (through monomer SOMO overlap) may also form in solution, which likely is higher in energy. As a result, the $(RCNSNS•)_2$ species in trans, cis, and staggered configurations may coexist in an equilibrium. Upon irradiation of the trans dimer $\mathbf{A}_2$ at 376 and 480 nm to an excited state ($\mathbf{A}_2$*), this trans dimer allows a concerted rearrangement via only a slight movement of all the atoms by the net cleavage of two S−C and N−S bonds and the gain of two C−N and S−S bonds per dimer, resulting in formation of the corresponding thermodynamically more stable (ca. 316 kJ/mol[21]) $\pi^*-\pi^*$ dimer $\mathbf{B}_2$ either in an excited or in a ground state. The structure of trans dimer $\mathbf{B}_2$ (Figure 1) is likely only slightly higher in energy than that observed in the solid state for cis $(PhCNSSN•)_2$[7a] and twisted $(RCNSSN•)_2$ (R = CH_3,[7b] CF_3;[7c] ca. 5 kJ/mol for R = CF_3), which in solution are in equilibrium with the monomers.[10] Rotomers of the $(RCNSNS•)_2$ dimers other than trans $\mathbf{A}_2$ are incompatible with the proposed concerted rearrangement. Reasonably, only the trans dimer undergoes the concerted photochemical rearrangement, and the other rotomers (cis and staggered) may only rearrange by this route on rapid equilibration to the trans dimer. The complete mechanism is summarized in eq 3. Thus we have

$$2\mathbf{A} \rightleftharpoons \mathbf{A}_2 \xrightarrow{h\nu} \mathbf{A}_2^* \rightarrow \mathbf{B}_2 \rightleftharpoons 2\mathbf{B} \qquad (3)$$

shown in this work that the isomerization of RCNSNS• to RCNSSN• proceeds by a photochemical rearrangement of the identified intermediate dimer in solution most likely in a concerted pathway.

Having established the nature of the radical dimers $\mathbf{A}_2$ and $\mathbf{B}_2$ and unambiguously proved the dimeric pathway of the rearrangement, we examined the electronic structures of the dimers $\mathbf{A}_2$ (R = H) and $\mathbf{B}_2$ (R = H) by CNDO calculations in order to fully understand the nature of the rearrangement. An inversion center is retained throughout the rearrangement; therefore, the MO's of $\mathbf{A}_2$ can be correlated with those of $\mathbf{B}_2$ with respect to *i* (Figure 8). Of the 27 occupied MO's (valence electrons only), $\mathbf{A}_2$ has 14 symmetric (g) and 13 antisymmetric (u) with respect to *i*, while $\mathbf{B}_2$ has only 13 occupied MO's that are symmetric (g) and 14 antisymmetric (u). Consequently, correlation of the MO's of $\mathbf{A}_2$ and $\mathbf{B}_2$ involves a crossover correlation between an occupied antibonding $\pi-\pi$ MO of $\mathbf{A}_2$ (A_g, SOMO-1) and a high energy unoccupied σ^* S−S MO of $\mathbf{B}_2$ (B_g) and between a high-energy unoccupied $\pi^*\text{-}\pi^*$ MO of $\mathbf{A}_2$ (A_u) and an occupied intermonomer σ S−S MO of $\mathbf{B}_2$ (B_u). Thus the rearrangement is photochemically symmetry allowed but thermally symmetry forbidden,[20] consistent with observed photochemically induced nature of the rearrangement. In addition, many of occupied low-lying $\pi\text{-}\pi$ MO's of $\mathbf{A}_2$ correlate with occupied low-lying σ-type S−S MO's of $\mathbf{B}_2$. Conceivably, the rearrangement proceeds by the allowed electronic transition from an occupied MO A_g to unoccupied MO A_u, which may be the origin of the absorption band of the $(RCNSNS•)_2$ dimer at 480 nm. The other dimer absorption band at 376 nm may originate from a transition to a higher unoccupied MO which then relaxes to the A_u level at 480 nm.

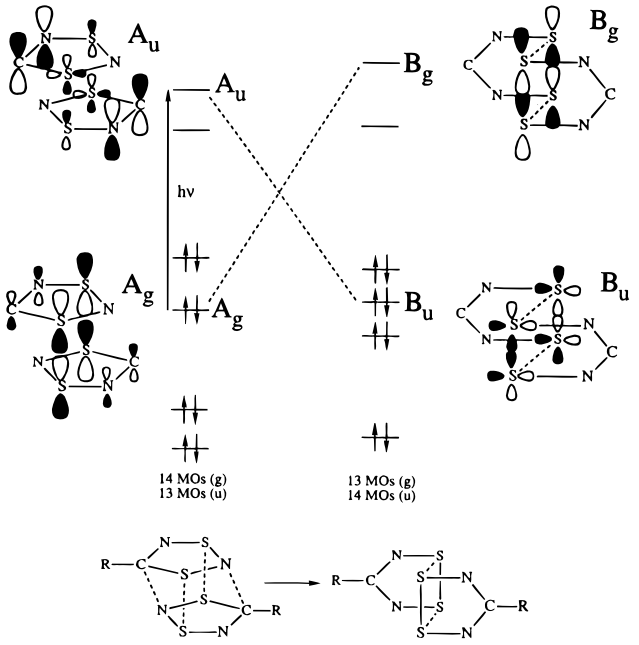

Figure 8. Correlation diagram of the molecular orbitals (CNDO) of the $(HCNSNS•)_2$ dimer and its rearrangement product $(HCNSSN•)_2$ dimer. The low-lying and some high unoccupied orbitals are omitted.

In addition to the photochemical rearrangement, we have previously observed that rearrangement also occurs at room temperature in the dark in dilute solution (e.g. for R = CF_3,[4] *p*-$O_2NC_6H_4$,[1f] and 3,5-$(O_2N)_2C_6H_3$[1f]) and in the solid state (for R = Ph and 3,5-$(ON)_2C_6H_3$[1f]) over extended periods of time. We have also noted that the thermal rearrangement of RCNSNS• (at a given concentration) in the dark was qualitatively faster the higher the electronegativity of R.[1f] This low-energy thermal rearrangement in the dark may also proceed via formation of an intermediate dimer $\mathbf{A}_2$, very likely in a concerted but a symmetry-disallowed process, consistent with the qualitatively slower rearranging rates[1f] in the dark.[23]

Conclusions

Our investigations show that in dilute solution the 1,3,2,4-dithiadiazolyl RCNSNS• radicals undergo two photochemically-symmetry allowed concerted processes, i.e. a dissociation to

RCN and likely SNS$^\bullet$ and a facile rearrangement to the thermodynamically more stable isomer 1,2,3,5-dithiadiazolyl RCNSSN$^\bullet$. The bimolecular (dimeric) rearrangement via dimer formation is supported (Figure 1 and eq 1) by the identification of the (RCNSNS$^\bullet$)$_2$ dimer (R = Ph, *p*-$O_2NC_6H_4$, 3,5-$(O_2N)_2C_6H_3$, CF_3) in solution and by its subsequent quantitative rearrangement on direct irradiation at its absorption frequencies (376 and 480 nm). The concerted rearrangement may occur with only minor displacement of atoms (Figure 1). CNDO studies of the dimer $\mathbf{A}_2$ and corresponding disulfide isomer $\mathbf{B}_2$ by a Woodward−Hoffmann analysis implies that the concerted rearrangement is thermally symmetry forbidden but photochemically symmetry allowed. This rearrangement resulting in the net exchange of the two adjacent atoms within a ring is unique, and our results show that it is a general process for 1,3,2,4-dithiadiazolyl radicals. To our knowledge, this is the first report of UV−visible spectroscopic studies of dithiadiazolyl radicals and the radical dimers (RCNSNS$^\bullet$)$_2$ (R = Ph, *p*-$O_2NC_6H_4$, 3,5-$(O_2N)_2C_6H_3$, CF_3) that have been directly observed in solution for the first time. A study of the kinetics of the rearrangement is in progress.

RCNSNS$^\bullet$ (R = Bu^t, Ph, 3,5-$(O_2N)_2C_6H_3$) not only undergo photochemical rearrangement but also undergo substantial first-order (in radical concentration) photolysis in normal room light to give RCN and presumably SNS$^\bullet$. Therefore, the photolysis can be reasonably regarded as a unimolecular process. This photolysis occurs almost quantitatively (for R = Bu^t and Ph) on irradiation at the absorption of RCNSNS$^\bullet$ monomer (254 nm) which was reasonably proposed to proceed via an excited dissociative state of RCNSNS$^\bullet$ on the basis of STO-3G calculations. The photolysis of RCNSNS$^\bullet$ may be an alternative route to a cleaner source of SNS$^\bullet$.[19]

Since RCNSNS$^\bullet$ radicals undergo facile rearrangement to the thermodynamically more stable RCNSSN$^\bullet$, the isolation of −CNSNS$^\bullet$ based radicals is generally not achieved. However, we were able to isolate derivatives of RCNSNS$^\bullet$ monoradicals with electron-donating R (R = CH_3,[2] Bu^t,[3] Ph[1f]). The very insoluble *p*-$O_2NC_6H_4$CNSNS$^\bullet$ [1f] (with an electronegative substituent) and various (CNSNS$^\bullet$)$_x$ ($x \geq 2$) species containing multiradicals[4−6] have also been prepared by isolating them in the solid state before the rearrangement could occur. For more electronegative R (R = CF_3,[2] I,[24] 3,5-$(O_2N)_2C_6H_3$[1f]), the reduction of RCNSNS$^+$ in the dark on a preparative scale led to the rapid formation of rearranged RCNSSN$^\bullet$ radicals, and isolation of the unrearranged RCNSNS$^\bullet$ was not achieved. For more electropositive R (R = Bu^t,[3] and Ph[1f]) the disulfides RCNSSN$^\bullet$ can be prepared by the photochemical rearrangement of RCNSNS$^\bullet$ in concentrated liquid SO_2 solution.[25] Our qualitative correlation between the rearrangement time of RCNSNS$^\bullet$ and the electronegativity of R can be employed as a guide to the preparation and isolation of RCNSNS$^\bullet$ and RCNSSN$^\bullet$ mono- and multiradicals. However, a complete understanding of the RCNSNS$^\bullet$ system has not been achieved. For example, the attempted preparation of 5-methyl-1,2,3,5-dithiadiazolyl CH_3CNSSN$^\bullet$ radical by the rearrangement of the corresponding 1,3,2,4-isomer CH_3CNSNS$^\bullet$ (ca. 0.1 M) in liquid SO_2 led to an insoluble material with a chemical analysis suggesting a mixture of products.[26]

Finally, we have made substantial progress in elucidating the mechanism of the novel rearrangement and in understanding the baffling nature of the 1,3,2,4-dithiadiazolyl RCNSNS$^\bullet$ radical system by simple experimental and theoretical studies. Many questions remain and await more comprehensive and sophisticated investigations.

Acknowledgment. We thank Dr. S. Mattar for important ESR spectroscopic measurements and Mr. Todd Way for simulating the UV−visible spectra of PhCNSNS$^\bullet$ by Quathro Pro (see Figure 5). Thanks are also expressed to Drs. F. Grein and W. V. F. Brooks for their very helpful discussions on the theoretical and physical chemical matters and to Dr. N. Burford of Dalhousie University for encouragement, reading the manuscript, and suggestions. In addition, we are indebted to Dr. N. Burford for his theoretical treatment of the rearrangement; see ref 3 and his extensive preliminary studies. Financial support from the NSERC (Canada) and University of New Brunswick is gratefully acknowledged.

Supporting Information Available: Change in height (*h*) of the most upfield peak in ESR spectra of Bu^{t}CNSNS$^\bullet$ with irradiation (at 254 nm) time (Figure S1), ESR spectra of the PhCNSNS$^\bullet$ radical at various temperatures (Figure S2), plot of the logarithm of the equilibrium constant (*K*) of PhCNSNS$^\bullet$ dimerization against the reciprocal of the absolute temperature (Figure S3), UV−visible spectrum of pure PhCNSSN$^\bullet$ in $CFCl_3$ (Figure S4), relationship between the absorbances of PhCNSNS$^\bullet$ at several wavelengths in the simulated UV−vis spectra and the square of the initial concentration of the PhCNSNS$^\bullet$ monomer (Figure S5), ESR parameters and concentrations of PhCNSNS$^\bullet$ at various temperatures (Table S1), and equilibrium constants of the dimerization of PhCNSNS$^\bullet$ at various temperatures (Table S2) (9 pages). Ordering information is given on any current masthead page.

IC9509140

(23) A preliminary kinetic study of the thermal rearrangement of 3,5-$(O_2N)_2C_6H_3$CNSNS$^\bullet$ (electronegative derivative) to 3,5-$(O_2N)_2C_6H_3$-CNSSN$^\bullet$ in dilute solution (0.02 M) in the dark showed that the reaction rate increased with time in the initial period, implying an autocatalysis process; i.e., the thermal rearrangement may also be catalyzed by a reaction product. For PhCNSNS$^\bullet$ (electropositive derivative), the rearrangement in dilute solution (0.02 M) did not occur in the dark at room temperature.

(24) The rearranged radical ICNSSN$^\bullet$ was characterized by elemental analysis and ESR (1:2:3:2:1 pentet): Burford, N.; Passmore, J.; Sun, X. Unpublished results.

(25) SO_2 has strong absorption in the UV region below 340 nm, which prevents the photolysis of RCNSNS$^\bullet$ to RCN, S_8, and N_2 under UV irradiation (maximum absorption 250 nm).

(26) Burford, N.; Passmore, J. Unpublished results.